Targeted Design of porous materials without strong, directional interactions

Megan O'Shaughnessy,[a] Peter R. Spackman, [b,c,d] Marc A.Little,[a] Luca Catalano,[a] Alex James,[a] Graeme M. Day, *[b] and Andrew I. Cooper*[a]

[a]*Materials Innovation Factory and Department of Chemistry, University of Liverpool, Liverpool, L7 3NY (UK),*

[b]*Computational System Chemistry, School of Chemistry, University of Southampton, Southampton, SO17 IBJ (UK)*

[c]*Leverhulme Research Centre for Functional Materials Design, Department of Chemistry and Materials Innovation Factory, University of Liverpool, Liverpool, L7 3NY, UK*

[d]*Curtin Institute for Computation, School of Molecular and Life Sciences, Curtin University, PO Box U1987, Perth, Western Australia 6845, Australia*

Table of Contents:

1.0 Computational Methodology

Geometry optimisation Crystal structure prediction was performed using a quasi-random sampling procedure, implemented in Global Lattice Energy Explorer (GLEE) software (version 2).[1] A search for molecular conformations was carried out using the Schrödinger Maestro package with the OPLS2005 [2] force field (no cut off and a dielectric constant of 1.0) using a mixed torsional/low-mode search. A maximum of 10000 steps were allowed and conformers with an energy less than 35 kJ mol-1 from the global minimum and with an RMSD in atomic positions of greater than 0.3 Å from all previously generated conformers were retained. Each conformer was subsequently geometry optimized using dispersion corrected (D3BJ)[3] density functional theory (DFT), using the B3LYP[4,5] functional with a 6-311G(d,p) basis.[6,7] Molecular DFT calculations were performed with the Gaussian09 software (Revision D).[8]

Redundant conformers (again, those with an RMSD < 0.3 Å) according to their DFT optimised gas-phase geometries were then eliminated. These gas-phase molecular geometries were then held rigid throughout crystal structure generation and lattice energy minimisation.

The relative energies of the final gas-phase conformations are available in Table S1, and their geometries are available in the supporting information.

Geometry optimisation in a polarisable continuum

Due to the plethora of low energy structures, relatively flat potential energy surface with regard to torsional changes, and the significant effect that the orientation of the sulfonyl chloride functional group has on crystal packing, we used a polarisable continuum model (PCM) with a sensible, if large, dielectric constant of 4.0 to mimic a molecular crystal-like environment. To this end, the previously described methodology for geometry optimisations was followed with the caveat that the self-consistent reaction field (SCRF) method was used. Specifically, the Integral equation formalism polarisable continuum model (IEFPCM), the default PCM method in Gaussian09 was utilised and, rather than using parameters for a solvent, we used a dielectric constant of Eps=4.0 and EpsInf=1.8. Atomic radii for the PCM surface were the defaults in Gaussian09, *i.e.*, UFF radii.

Total SCF energies are not directly comparable between gas-phase calculations and SCRF calculations, so in order to compare the energetic penalty associated with the PCM conformations the lowest energy conformer from the PCM set was fixed and a single-point energy calculated with the same procedure as the gas-phase geometries. Using this procedure, the gas-phase conformer was approximately 3 kJ/mol lower than the lowest PCM conformer.

Likewise, the difference between the conformer from the lowest energy structure matching the experimental crystal structure, and the lowest energy gas-phase conformer found was only roughly 5 kJ/mol.

The relative energies of the final conformations of the conformers optimised in a crystal-like dielectric are available in Table S1, and their geometries are available in the supporting information. For the CSP datasets see DOI: https://doi.org/10.5258/SOTON/D2313

Table S1 Relative energies (kJ/mol) of conformers used in the CSP within this study. The Relative Energy column is as compared to the minimum energy conformer in each category (PCM vs. Gas-Phase).

Crystal-like dielectric (ε = 4)		Gas-Phase	
Conformer ID	**Relative Energy (kJ/mol)**	**Conformer ID**	**Relative Energy (kJ/mol)**
90	0.00	22	0.00
89	0.36	26	0.03
77	0.46	24	0.03
75	0.46	25	0.03
71	0.46	29	0.07
72	0.46	38	0.07
67	0.46	28	0.07
78	0.46	35	0.07
68	0.46	34	0.07
81	0.46	27	0.07
70	0.46	36	0.07
69	0.46	32	0.07
87	0.46	33	0.07
80	0.46	30	0.07
73	0.46	37	0.07
76	0.46	31	0.07
82	0.46	19	0.08
30	0.53	18	0.19
41	0.53	16	0.20
40	0.53	20	0.20
11	0.80	1	0.42
5	0.82	9	0.46
6	0.86	7	0.46
10	0.86	6	0.46
17	0.86	4	0.46
15	0.86	8	0.46
24	0.86	3	0.46
26	0.86	10	0.46
28	0.86	12	0.46
21	0.86	2	0.46
14	0.86	11	0.46
7	0.89	5	0.46
52	1.28	21	0.66
1	1.39	39	1.11
34	1.43	13	1.75
		15	2.63
		14	2.91
		17	2.93
		23	2.96

Table S2 Root-mean-square deviation (RMSD, in Å) of gas-phase vs. crystal-like dielectric optimised conformers used in the CSP within this study. None of the PCM optimised conformations correspond to any of the gas-phase conformations.

Crystal-like dielectric ($\epsilon = 4$) optimised conformer ID	Gas-phase optimised conformer ID																
	1	**3**	**4**	**7**	**10**	**11**	**12**	**13**	**14**	**15**	**20**	**24**	**26**	**27**	**31**	**38**	**39**
1	1.18	0.94	1.32	0.94	1.32	1.76	1.76	1.87	1.94	1.76	1.79	1.66	1.66	1.69	1.20	1.20	1.20
5	0.57	1.41	0.85	1.41	0.85	1.41	0.85	1.24	0.92	1.49	1.02	1.46	1.01	1.52	1.65	1.59	1.76
6	1.66	1.59	1.69	1.59	1.61	0.93	4.76	0.60	0.74	0.76	1.49	0.72	1.47	0.92	0.92	1.23	1.02
7	0.72	1.55	0.94	1.56	0.95	1.54	1.71	4.73	1.92	1.61	1.62	1.65	1.61	1.62	1.51	1.57	1.31
10	0.70	1.43	0.93	1.56	0.47	1.61	1.59	4.73	1.84	1.54	1.63	1.61	1.49	1.58	1.51	1.52	1.32
11	0.59	1.56	0.83	1.43	0.83	1.40	1.58	1.58	1.77	1.46	1.46	4.87	1.47	1.43	1.41	1.42	1.50
14	0.64	4.92	0.32	1.51	0.88	1.64	0.88	1.34	0.91	1.61	0.66	1.53	1.05	1.49	1.47	1.46	1.59
15	1.46	0.47	4.76	0.93	1.43	0.94	1.56	1.02	1.09	1.10	1.62	1.10	1.60	1.23	1.57	1.66	1.73
17	1.46	0.47	4.76	0.93	1.43	1.72	1.68	1.71	1.89	1.57	1.63	1.64	1.59	1.69	0.92	0.92	1.02
30	0.92	1.47	0.75	1.47	0.75	1.60	1.10	1.31	0.97	1.55	0.94	1.65	1.24	1.56	1.54	1.62	1.71
34	1.78	1.78	1.78	1.66	1.63	1.19	1.00	1.08	0.84	1.32	1.14	1.04	0.81	1.14	1.36	1.36	0.99
40	0.92	1.47	0.75	1.47	0.75	1.62	1.48	1.68	1.81	1.59	1.51	1.65	1.59	1.62	1.41	1.41	1.19
52	1.12	1.18	1.27	1.39	1.02	1.38	1.02	1.07	0.84	1.30	1.15	1.26	1.13	1.35	1.76	1.79	1.84
67	1.10	1.48	0.97	1.47	0.96	1.55	1.54	1.71	1.83	1.58	1.57	1.61	1.56	1.65	1.43	1.25	1.00
68	1.10	1.48	1.26	1.62	0.98	1.47	0.96	1.36	1.10	1.57	1.12	1.37	0.76	1.43	1.70	1.65	4.79
69	1.52	0.98	1.62	1.26	1.48	1.57	1.64	1.73	1.87	1.59	1.69	1.61	1.65	1.65	0.95	0.95	0.59
70	1.52	0.97	1.48	0.96	1.47	1.56	1.57	1.61	1.78	1.47	1.52	1.56	1.61	1.61	0.94	0.49	0.59
71	1.10	1.47	0.96	1.48	0.97	1.67	1.58	4.80	1.85	1.66	1.59	1.65	1.67	1.74	1.25	1.43	1.00
73	1.52	0.96	1.47	0.97	1.48	1.63	1.61	1.70	1.79	1.62	1.50	1.67	1.65	1.71	0.50	0.94	0.59
82	1.10	1.62	0.98	1.48	1.26	1.48	0.97	1.14	0.74	1.44	0.79	1.37	0.76	1.25	1.59	1.54	4.79
89	1.28	1.46	1.17	1.46	1.17	1.61	1.61	1.76	1.83	1.61	1.67	1.59	1.59	1.69	1.22	1.22	0.69
90	1.58	1.12	1.52	1.12	1.53	1.12	1.52	0.85	0.89	1.01	1.44	0.96	1.43	0.76	1.60	1.65	1.83

2.0 Materials and Methods

Materials: Tetraphenylmethane was purchased from Manchester Organics. All other chemicals were purchased from Sigma-Aldrich and used as received, except for chlorosulfonic acid which was distilled prior to use.

NMR: ^{1}H and ^{13}C NMR spectra were recorded at 400 MHz on a Bruker Advance 400 NMR spectrometer. Chemical shifts are reported in ppm with reference to internal residual protonated species of the deuterated solvents used for ^{1}H and ^{13}C analysis.

Fourier-transform infrared spectroscopy (FT-IR): FT-IR spectra were recorded on a Bruker Tensor 27 FT-IR spectrometer using bulk solid sample and an ATR attachment (16 scans).

Thermogravimetric Analysis (TGA). TGA was carried out using a Q5000IR (TA Instruments) with an automated vertical overhead thermobalance. Samples (3 – 5 mg) were heated in platinum pans at a rate of 10 °C/min unless stated otherwise.

Powder X-ray Diffraction (PXRD): PXRD data were collected in transition mode on powder samples held on thin Mylar film in aluminium well plates on a Panalytical Empyrean diffractometer equipped with a high throughput screening XYZ stage, X-ray focusing mirror, and PIXcel detector, using Cu-Kα (λ = 1.541 Å) radiation.

Single Crystal X-ray Crystallography: Single crystal X-ray data were measured on a Rigaku MicroMax-007 HF rotating anode diffractometer (Mo-Kα radiation, λ = 0.71073 Ã, Kappa 4-circle goniometer, Rigaku Saturn724+ detector). Rigaku frames were converted to Bruker compatible frames using the programme ECLIPSE.[9] Absorption corrections, using the multi-scan method, were performed with the programme SADABS.[10] The structure was solved with SHELXT,[11] and refined by full-matrix least-least square on $[F]^2$ SHELXL,[12] interfaced through the program OLEX2.[13] H atom positions for the C-H groups were refined using the riding model. For full refinement details, see supporting CIF files.

Gas Sorption Analysis: Nitrogen isotherms were collected at 77K using an ASAP2420 volumetric adsorption analyser (micrometrics instruments Corporation). Carbon dioxide isotherms were collected up to a pressure of 1200 mbar on a micrometrics ASAP2020 volumetric adsorption analyser at 298K and 273K. Carbon dioxide isotherm at 198K and Methane isotherms at 273K were collected using Micromeritics 3flex volumetric adsorption analyser.

Synthesis of Tetrakis(4-sulfonylchloridephenyl)methane (TSCl)

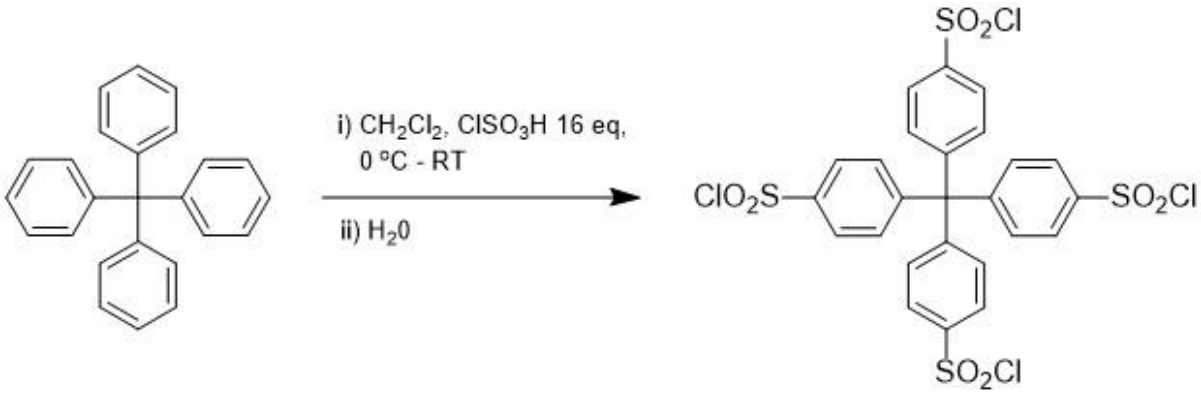

Scheme S1 The synthetic route used to form **TSCl**.

TSCl synthetic procedure: Tetraphenylmethane (1.5 g, 4.68 mmol) was dissolved in anhydrous CH_2Cl_2 (40 mL) under an inert N_2 atmosphere. Freshly distilled chlorosulfonic acid (1.25 mL, 18.72 mmol, 4 eq) was added dropwise over 1 hour with stirring at 0 °C then left for 1 hour before another 4 eq of freshly distilled chlorosulfonic acid was added in the same manner as previously. In total 16 eq of acid was added, after all the acid had been added the now thick brown suspension of solid was slowly warmed up to RT. The mixture was left stirring overnight to give a clear deep red solution with a small layer of black oil at the bottom of the round bottom flask. The deep red solution was slowly added dropwise to ice which resulted in the precipitation of a yellow solid, once all the ice had melted the yellow precipitate was filtered off and left on the filter paper for drying for 30 minutes to give the final product (1.83 g, 82% yield). ^{1}H NMR (400 MHz, DMSO-d_6, δ (ppm)): 7.54 (d, J = 8 Hz, 8H), 7.08 (d, *J* = 8 Hz, 8H). ^{13}C NMR (100 MHz, DMSO-d_6, δ (ppm)): 146.85, 145.86, 130.46, 125.52, 64.34. IR: v 1585, 1375, 1173, 1006, 826, 559. Anal. Cald. for $C_{25}H_{16}Cl_4O_8S_4$: C 42.03, H 2.26, S 17.95; Found C 41.76, H 2.25, S 17.64

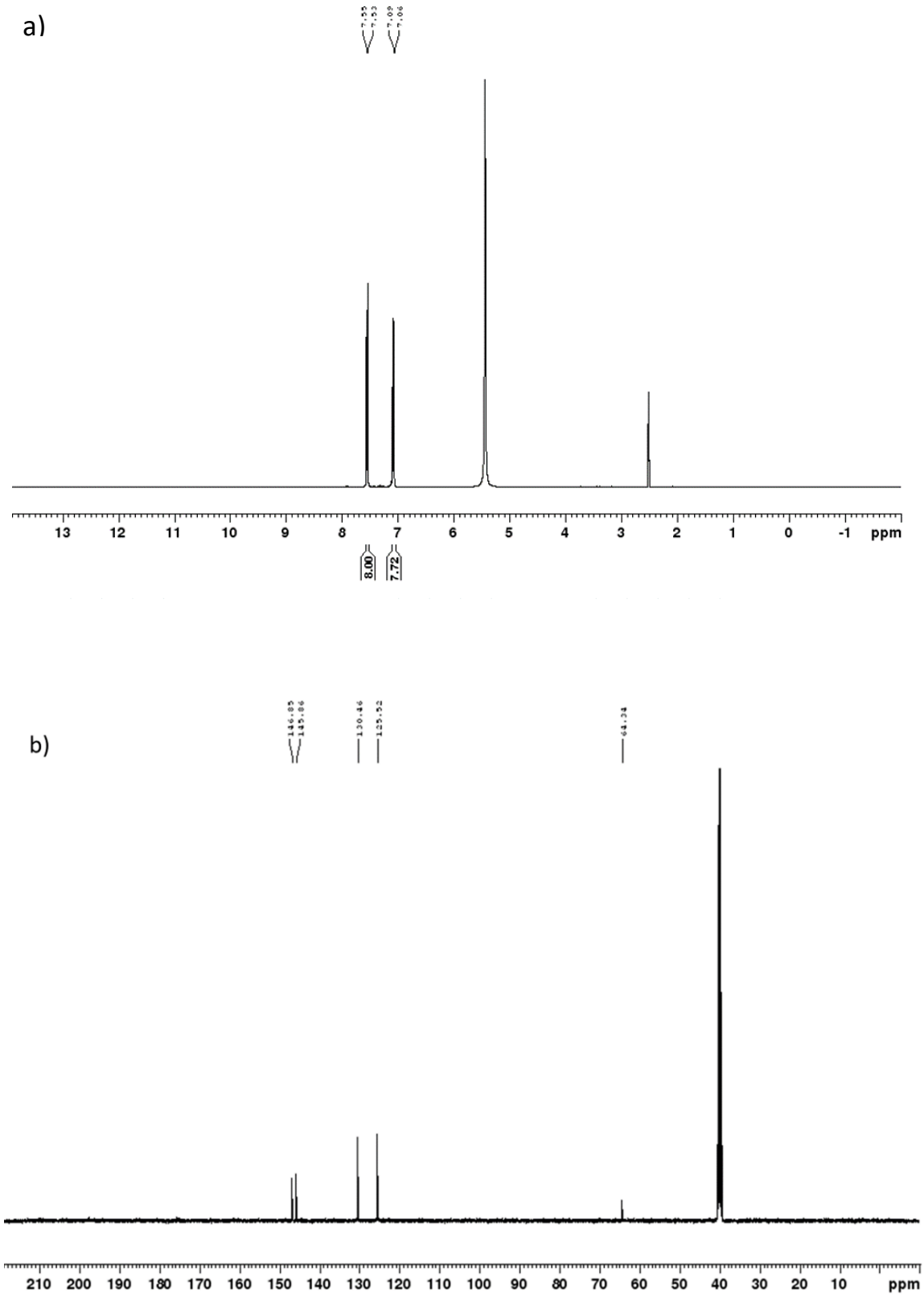

Figure S1. a) ^{1}H NMR (400 MHz, DMSO-d_6), and b) ^{13}C NMR (100 MHz, DMSO-d_6) spectra of **TSCl**.

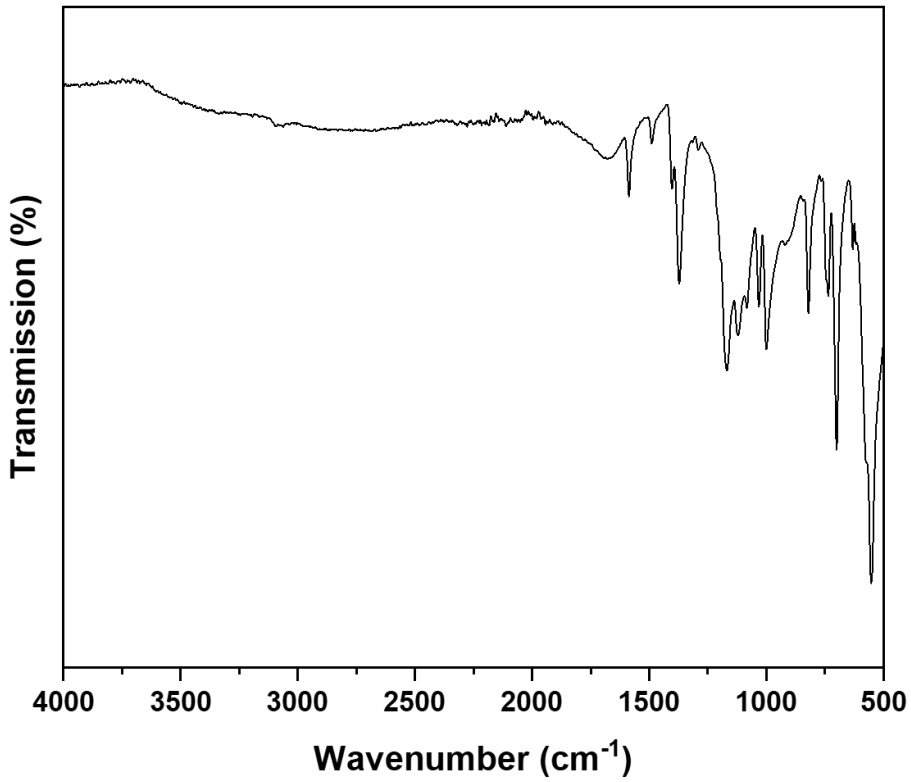

Figure S2. FT-IR spectra for **TSCl**

Crystallisation of TSCl

TSCl was shown by PXRD to form directly from the reaction as a bulk powder see **Figure S4**. Single crystals of **TSCl** suitable for x-ray diffraction were obtained by dissolving **TSCl** (40 mg) in 1,1,1,3,3,3-hexafluoropropanol (HFP) (10 mL) the solvent was then left to slowly evaporate off to give colourless block shaped crystals of **TSCl** within 3 days. The same method could be used to grow single crystals of **TSCl** in THF and ethyl acetate. To form bulk solid for gas adsorption and analysis which could be easily activated, **TSCl** (225 mg) was dissolved in HFP (60 mL) then Methyl acetate (20 mL) was added and the solution was swirled by hand to allow mixing of the solvents which resulted in an instant precipitation of powder. The powder was placed in a gas sorption tube and nitrogen was blown over it before it was activated by holding under vacuum at room temperature overnight on the gas port.

The crystal refinement data for **TSCl** (CCDC entry code: 2192388) is shown in Table S3. For a displacement ellipsoid plot of the asymmetric unit, see Figure S3.

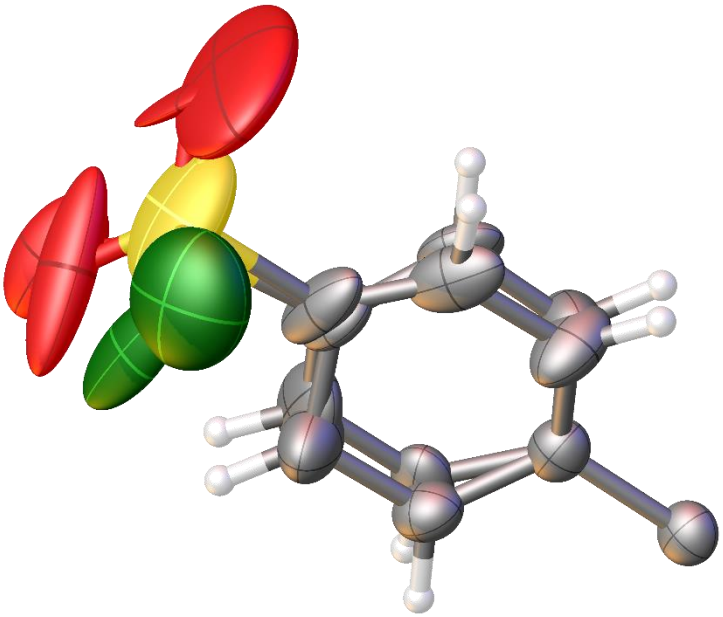

Figure S3. Displacement ellipsoid plot from the single crystal structure of **TSCl** showing one complete **TSCl** molecule, shown without the disorder for clarity. Ellipsoids are displayed at a 50% probability level. C: grey, S: yellow, O: red, Cl: green, H: white.

Table S3. Single crystal X-ray refinement details for solvated **TSCl**

Molecule	**TSCl**
λ [Å]	0.71073
Collection Temperature	100 K
Formula	$C_{25}H_{16}Cl_4O_8S_4$
Mr [g mol-1]	714.42
Crystal Size [mm]	0.127 x 0.107 x 0.07
Crystal System	Tetragonal
Space Group	*I*4
a [Å]	13.6104(8)
c [Å]	9.8000(5)
V [Å^3]	1815.4(2)
Z	2
D_{calcd} [g cm^{-3}]	1.307
μ [mm^{-1}]	0.595
F(000)	724
2θ range [°]	5.122 – 52.724
Reflections collected	10185
Independent reflections , R_{int}	1842, 0.0382
Obs. Data [$I > 2\sigma(I)$]	1647
Data /restraints / parameters	1842/ 209 / 175
Final R_1 values ($I > 2\sigma(I)$)	0.0483
Final R_1 values (all data)	0.0541
Final w$R(F_2)$ values (all data)	0.1345
Goodness-of-fit on F^2	1.095
Largest difference peak and hole [e.A^{-3}]	0.333 / -0.219
CCDC	2192388

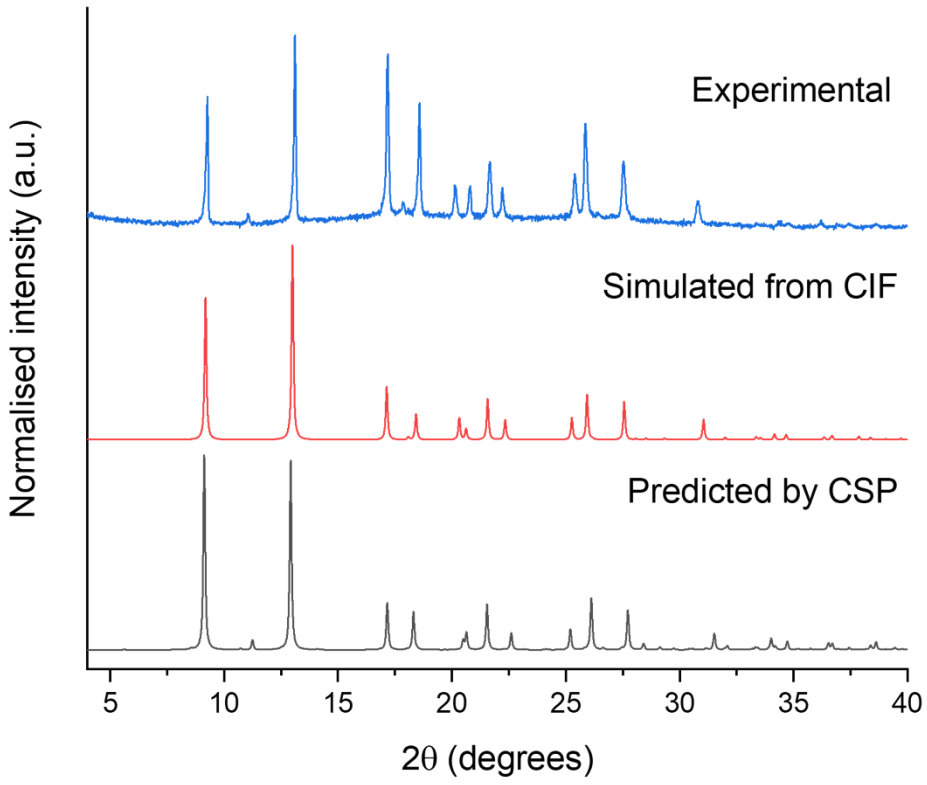

Figure S4. PXRD pattern for **TSCl** recorded from the bulk yellow powder obtained straight from the reaction mixture without further recrystallisation or purification. This is compared to the simulated PXRD from the single crystals and the predicted PXRD pattern for the structure from the CSP.

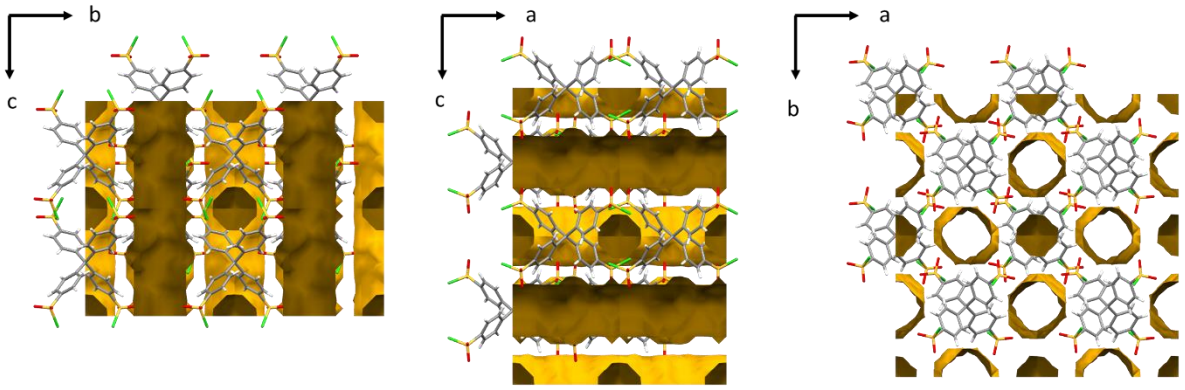

Figure S5. Crystal packing of **TSCl** from single crystal shown down the *a* and *b* axis. Surface contact voids are shown in yellow using probe radius of 1.55 Å, the Van der Waals radius of N_2 and grid spacing of 0.7 Å.

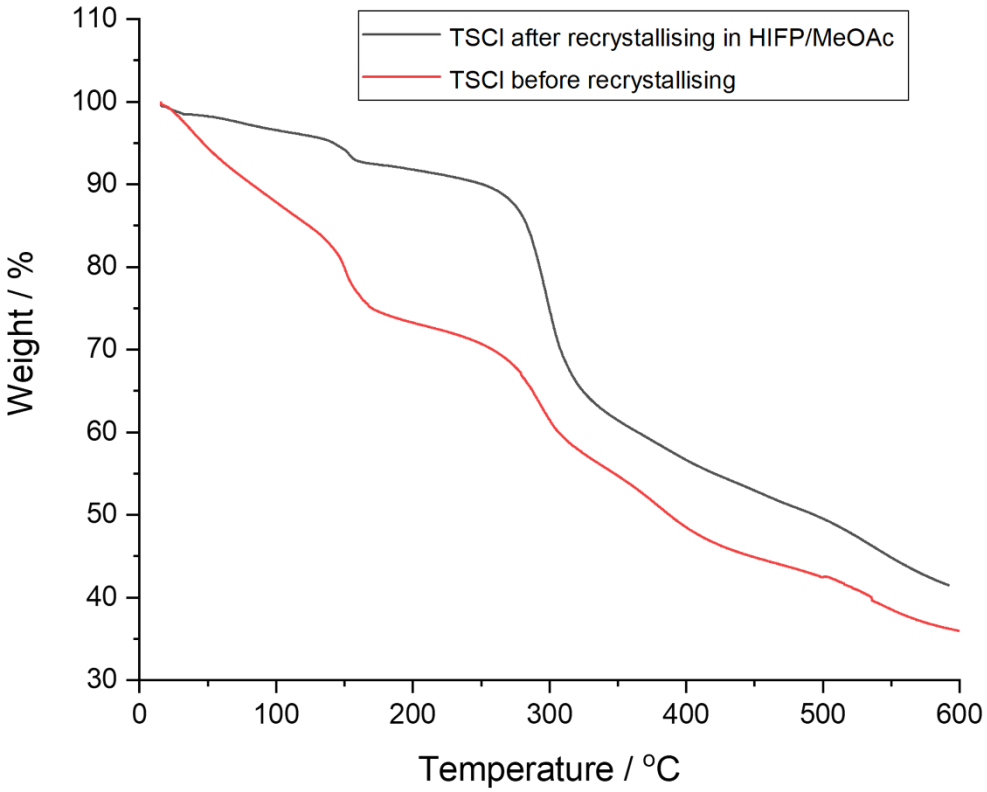

Figure S6. TGA trace of **TSCl** after isolating in its porous form straight from the reaction (red line). TGA trace of **TSCl** after recrystallising in HIFP/MeOAc before allowing the residual solvent molecules to evaporate out of the pores (black line).

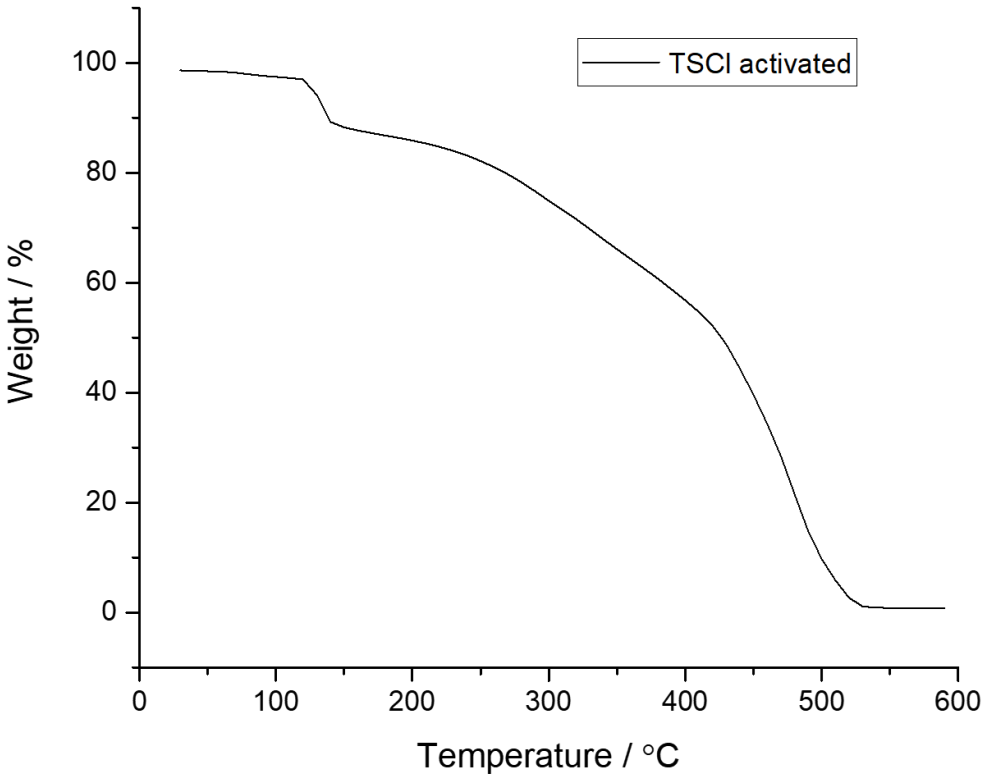

Figure S7. A TGA trace of activated **TSCl** showing a weight loss of ~3 wt.% before 140°C, which is likely to be physisorbed water in the pores.

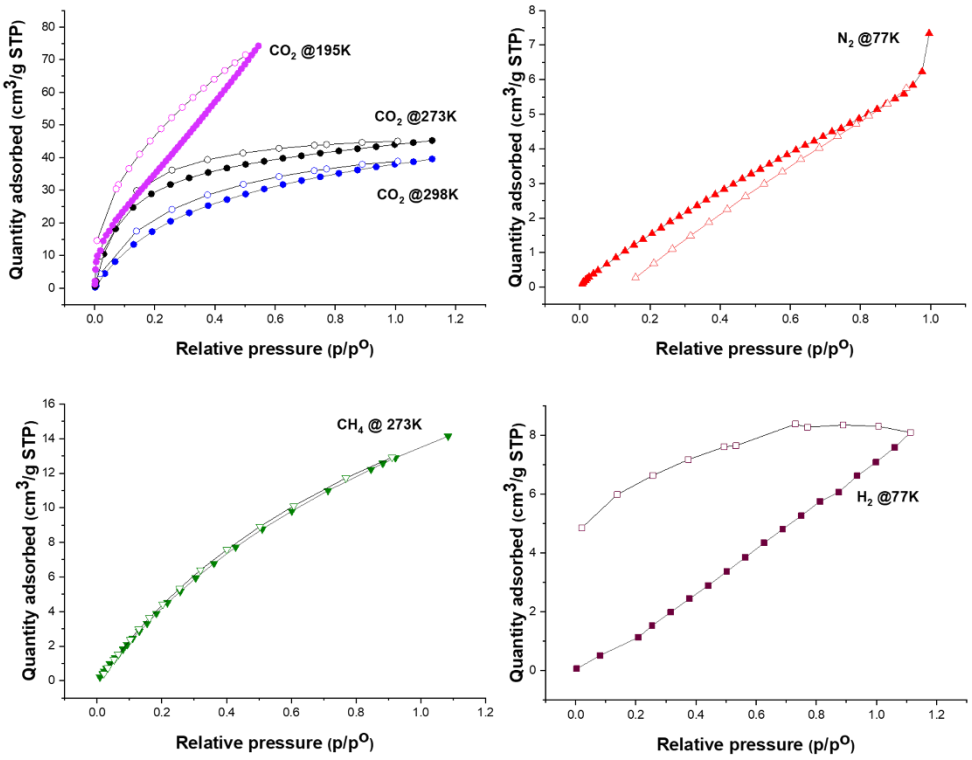

Figure S8. Gas sorption isotherms for **TSCl**, a) CO_2 at 195, 273, and 298 K. b) N_2 at 77 K, c) CH_4 at 273 K, and H_2 at 77 K. Closed symbols are for adsorption points, while open symbols are for the desorption points.

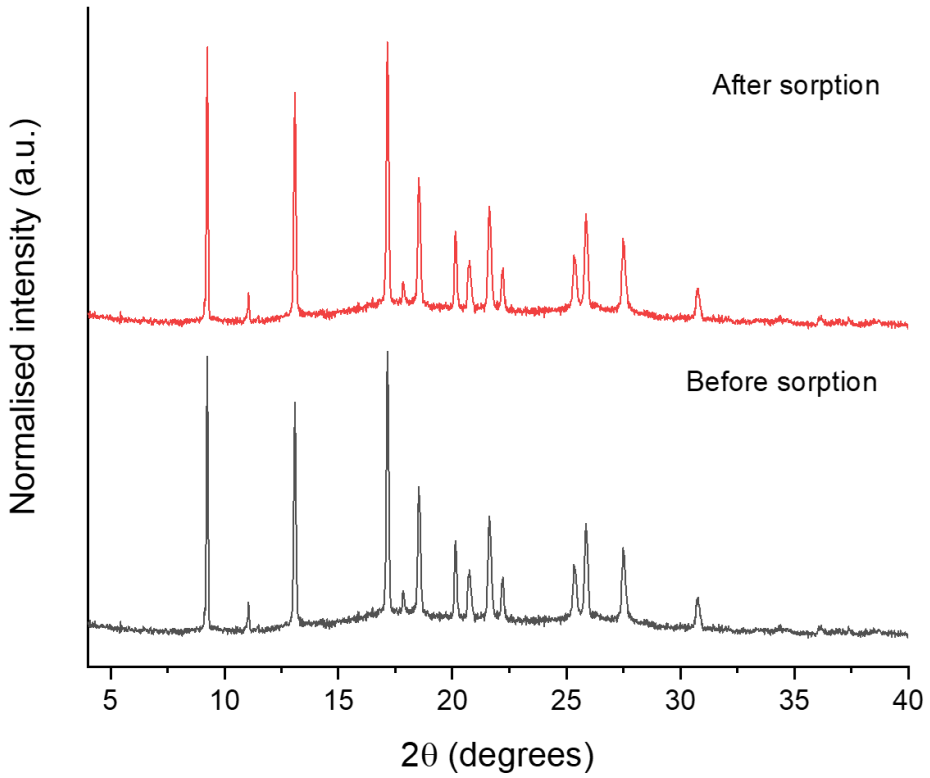

Figure S9. PXRD pattern for **TSCl** recorded before and after gas sorption cycles indicating no change in the structure after the sorption cycles.

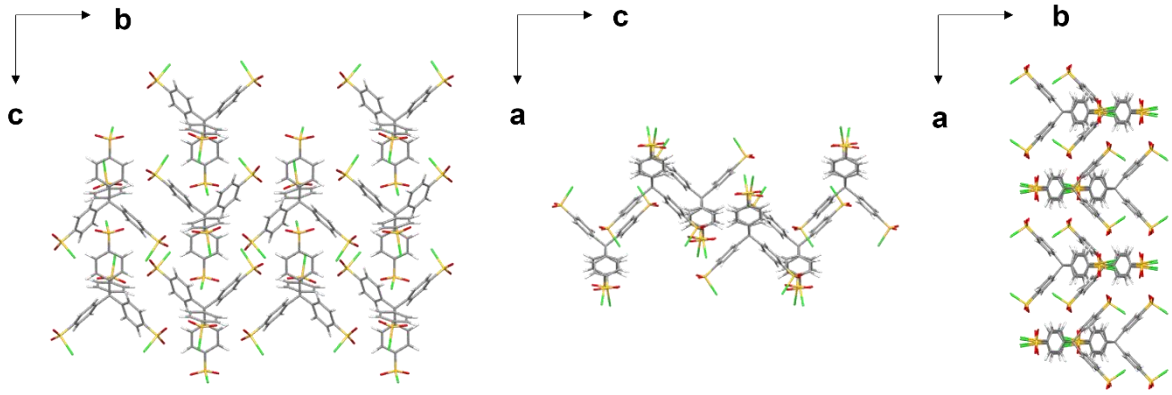

Figure S10. Crystal structure of the lowest energy crystal structure predicted by CSP.

Other reported sulfonyl chlorides reported in literature.

Searching the CSD database for crystals with the motif Ph-SO2Cl ··· O (Figure S9) gave 7 results for which the molecules can be seen in Figure S10. All these molecules pack densely together with no

channels. Some of the structures are packed using halogen bonding between the sulfonyl chloride groups, while others are packed through other intermolecular interactions such as hydrogen bonding and π- π stacking with there being halogen bonding between the two sulfonyl chloride groups within the same molecule. The packing of these molecules can be seen in Figure S11.

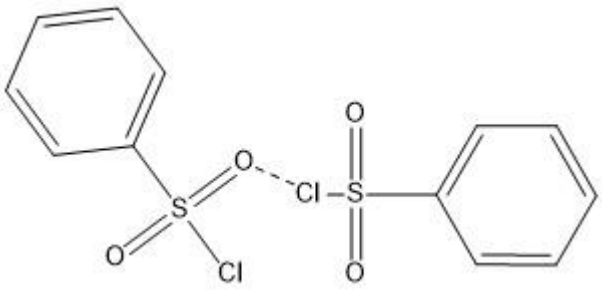

Figure S11. Structure of motif used to search for crystal structures containing sulfonyl chloride functional groups attached to a benzene ring. (Ph-SO2Cl ··· O)

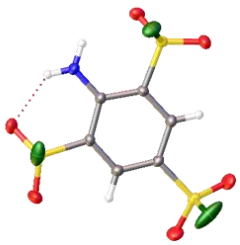 CCDC: 218411	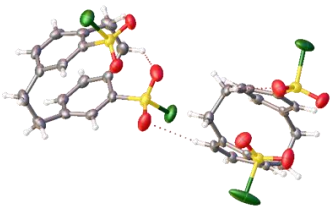 CCDC: 631112	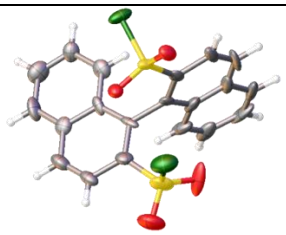 CCDC: 721091
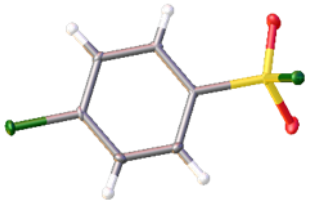 CCDC: 1005327	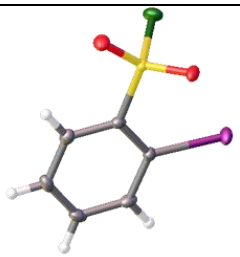 CCDC: 298482	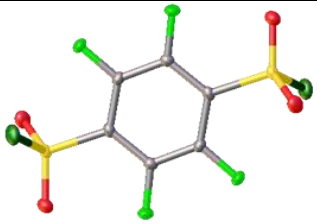 CCDC: 776936
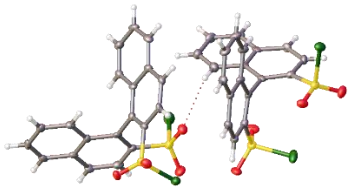 CCDC: 721092		

Figure S12. Showing the structures of the 7 results[14-16] found when searching the CSD database for the mofit Ph-SO2Cl ··· O.

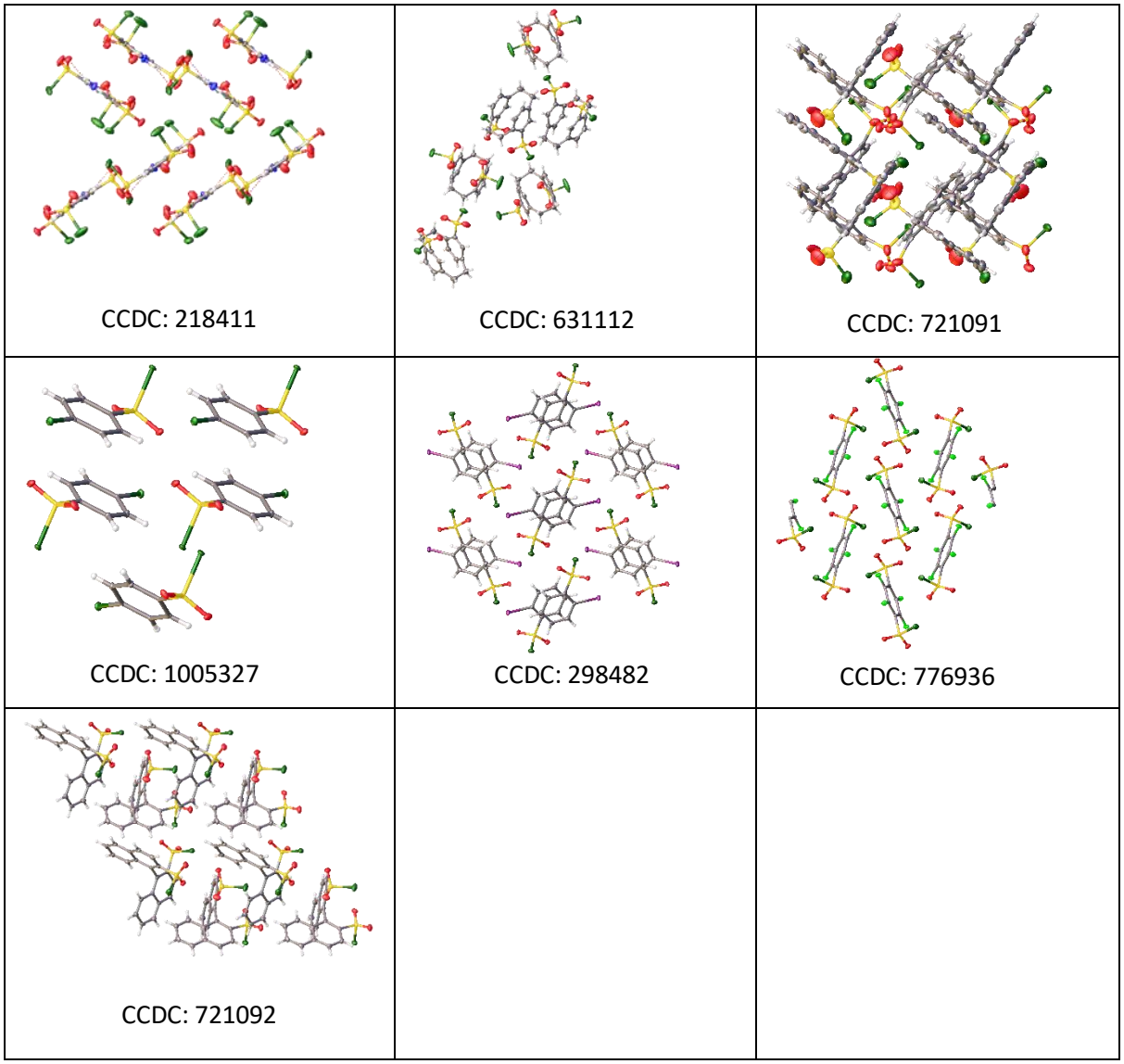

Figure S13. Packing of the 7 molecules seen in Figure S10. Images show the dense packing of the structures along with their corresponding CCDC reference number.

Stability tests of activated TSCl

While **TSCl** was shown in the original submission to be stable to activation, as shown by the gas isotherms, this does not prove its long-term stability to air / moisture over time.

The stability of solvated samples from the recrystallisations (HFIP/MeOAc) appeared good. PXRD data taken for samples left in a capped vail after 1 year showed no change. These samples were stored in the vials and were not under an inert atmosphere, but they were also not exposed to atmospheric air. To check the stability of an activated sample, it was placed into a well on a PXRD plate and the pattern was collected each day at roughly the same time to monitor any changes. The PXRD pattern for the

activated **TSCl** sample showed that after 5 days open to air, the crystallinity began to decrease (see Fig. S14, below). The now semi-crystalline sample was recrystallised, which gave the **TSCl** structure back with high crystallinity. This indicated that the material had begun to become disordered, rather than being chemically hydrolysed. This is in keeping with the fact that **TSCl** was isolated from water where it was shown to be stable to hydrolysis for at least 6 hours.

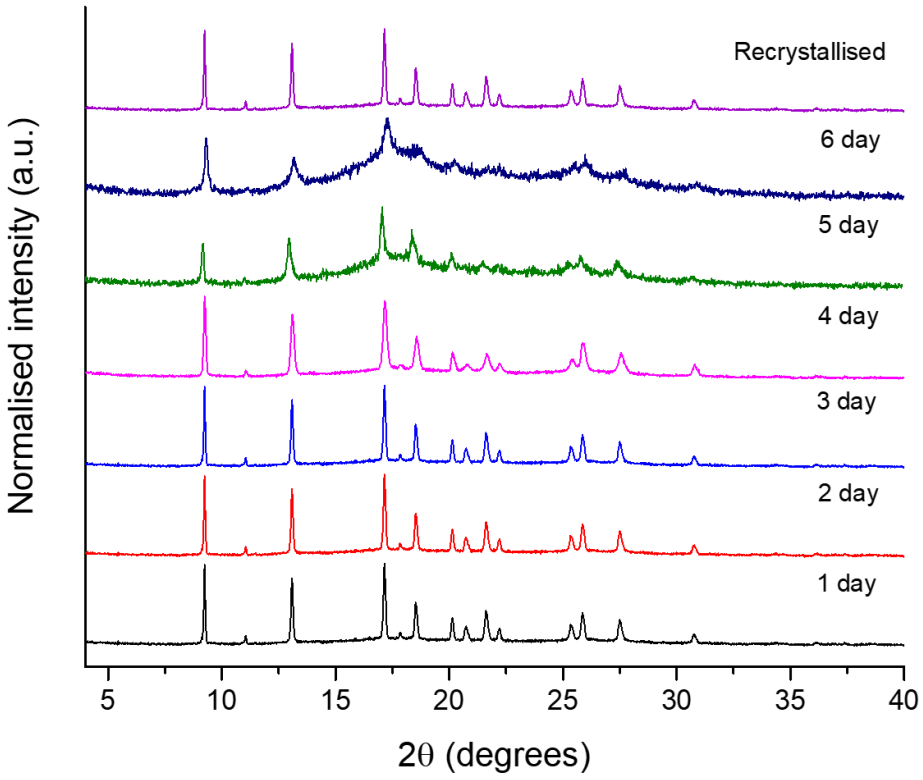

Figure S14. PXRD patterns of an activated sample of TSCl exposed to air over a period of 6 days, with the sample being recrystallised again after this period to achieve the same level of crystallinity (purple pattern, top).

To further test the stability of **TSCl** to hydrolysis, samples obtained from the recrystallisation both activated and unactivated were stirred in water at both room temperature and at 80 °C at a concentration of 5 mg/ml. The results of the tests can be seen in Table SI 4. In general, both the activated and solvated samples show more resilience to hydrolysis at room temperature, with the samples remaining stable for over 4 days. Both samples were hydrolysed at a faster rate when heated. Even with heating, there was no noticeable difference in the rate of hydrolysis for both samples and both were observed to dissolve in 10 -11 hours. To assess whether the material had been hydrolysed,

the sample was visually checked to see when it dissolved (which indicated that it had been converted to the corresponding sulfonic acid). The resulting solution was then freeze-dried and this powder analysed by PXRD. A sample of **TSCl** was first freeze-dried separately to check that it was stable under these conditions. These results showed that the structure transforms to a known polymorph of tetrakis(4-sulfophenyl)methane that has been previously reported.[17] Figure SI 15 shows the change in the PXRD pattern after hydrolysis. Table S4 shows the general trends in stability for **TSCl**.

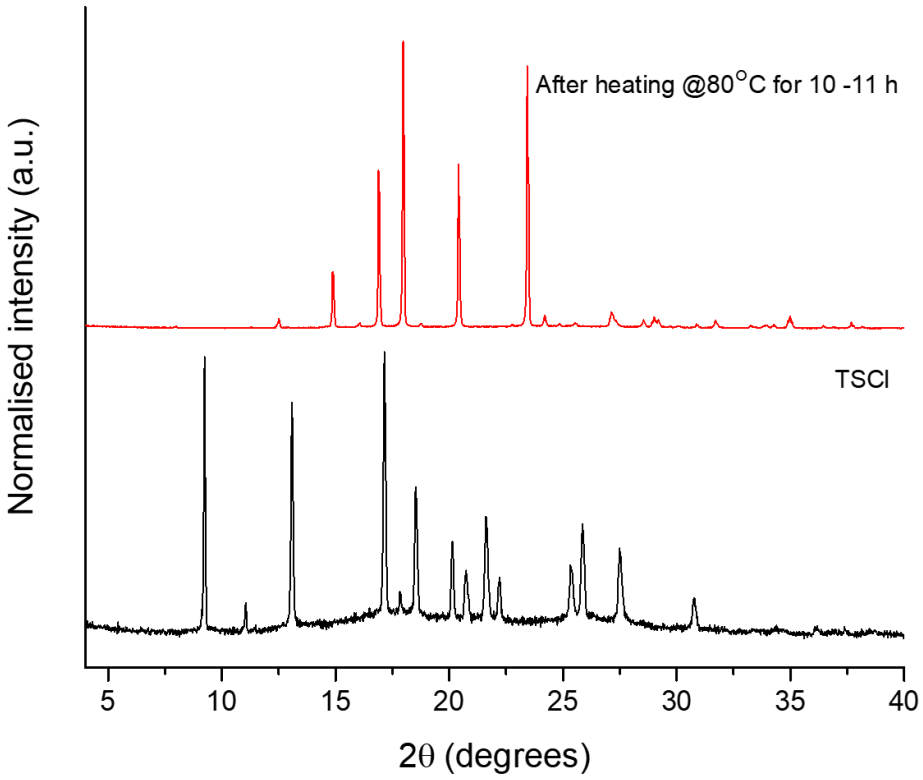

Figure S15. PXRD pattern for the activated sample of **TSCl** both before and after heating in water at 80°C for 10-11 hours, whereupon the structure has transformed to tetrakis(4-sulfophenyl)methane.

Table S4. General trend in the hydrolytic stability of **TSCl**.

Sample	Conditions	Time	Results
Solvated	Capped vial	1 year +	No change
Solvated	H_20 @ RT (5mg/ml)	4 days	No change
Activated	H_20 @ RT (5mg/ml)	4 days	No change
Solvated	H_20 @ 80 °C (5mg/ml)	~10 -11 hours	Hydrolysed
Activated	H_20 @ 80 °C (5mg/ml)	~10 -11 hours	Hydrolysed
Activated	Open to air	6 days	Loss of crystallinity

References

1. D. H. Case, J. E. Campbell, P. J. Bygrave and G. M. Day, *J. Chem. Theory Comput.* 2015, **12**, 910.
2. J. L. Banks, H. S. Beard, Y. Cao, A. E. Cho, W. Damm, R. Farid, A. K. Felts, T. A. Halgren, D. T. Mainz, J. R. Maple, R. Murphy, D. M. Philipp, M. P. Repasky, L. Y. Zhang, B. J. Berne, R. A. Friesner, E. Gallicchio and R. M. Levy, *J. Comp. Chem.* 2005, **26**, 1752.
3. S. Grimme, S. Ehrlich and L. Goerigk, *J. Comp. Chem.* 2011, **32**, 1456.
4. A. D. Becke, *J. Chem. Phys.* 1993, **98**, 5648.
5. P. J. Stephens, F. J. Devlin, C. F. Chabalowski and M. J. Frisch, *J. Phys. Chem.* 1994, **98**, 11623.
6. A. D. McLean and G. S. Chandler, *J. Chem. Phys.* 1980, **72**, 5639.
7. R. Krishnan, J. S. Binkley, R. Seeger and J. A. Pople, *J. Chem. Phys.* 1980, **72**, 650.
8. M. J. Frisch, G. W. Trucks, H. B. Schlegel, G. E. Scuseria, M. A. Robb, J. R. Cheeseman, G. Scalmani, V. Barone, B. Mennucci, G. A. Petersson, H. Nakatsuji, M. Caricato, X. Li, H. P. Hratchian, A. F. Izmaylov, J. Bloino, G. Zheng, J. L. Sonnenberg, M. Hada, M. Ehara, K. Toyota, R. Fukuda, J. Hasegawa, M. Ishida, T. Nakajima, Y. Honda, O. Kitao, H. Nakai, T. Vreven, J. A. Montgomery, Jr., J. E. Peralta, F. Ogliaro, M. Bearpark, J. J. Heyd, E. Brothers, K. N. Kudin, V. N. Staroverov, R. Kobayashi, J. Normand, K. Raghavachari, A. Rendell, J. C. Burant, S. S. Iyengar, J. Tomasi, M. Cossi, N. Rega, J. M. Millam, M. Klene, J. E. Knox, J. B. Cross, V. Bakken, C. Adamo, J. Jaramillo, R. Gomperts, R. E. Stratmann, O. Yazyev, A. J. Austin, R. Cammi, C. Pomelli, J. W. Ochterski, R. L. Martin, K. Morokuma, V. G. Zakrzewski, G. A. Voth, P. Salvador, J. J. Dannenberg, S. Dapprich, A. D. Daniels, Ö. Farkas, J. B. Foresman, J. V. Ortiz, J. Cioslowski, and D. J. Fox, Gaussian 09, Revision D.01. Gaussian, Inc., Wallingford CT, 2009.
9. S. Parsons, *Univ. Edinburgh, Edinburgh, UK*.
10. G. M. Sheldrick, SADABS, *University of Göttingen, Germany*, 2008.
11. G. Sheldrick, *Acta Cryst*. 2015, **A17**, 3.
12. G. Sheldrick, *Acta Cryst*. 2015, **C71**, 3.
13. O. V. Dolomanov, L. J. Bourhis, R. J. Gildea, J. A. K. Howard and H. Puschmann, *J. Appl. Cryst.* 2009, **42,** 339.

14. H. Christoph, J. Grunenberg, H. Hopf, I. Dix, P. G. Jones, M. Scholtissek and G. Maier, *Chem. Eur. J.* 2008, **14**, 5604.

15. M. Treskow, J. Neudörfl and R. Giernoth, *Eur. J. Org. Chem.* 2009, 3693–3697.

16. S. D. Robertson, A. M. Z. Slawin and J. D. Woollins, *Acta Cryst.* 2006, **E62**, 744.

17. B. Sarma and A. Nangia, *CrystEngComm*, 2007, **9**, 628.